ELSEVIER

International Journal of Mass Spectrometry 222 (2003) 269–279

International Journal of Mass Spectrometry

www.elsevier.com/locate/ijms

The energetics of nitric oxide generation upon protonation of diazeniumdiolates

Loubna A. Hammad[a], Patrick H. Ruane[b], Neema A. Kumar[b], John P. Toscano[b], Paul G. Wenthold[a,*]

[a] *Department of Chemistry, Purdue University, West Lafayette, IN 47907-1393, USA*
[b] *Department of Chemistry, Johns Hopkins University, Baltimore, MD 21218, USA*

Received 30 April 2002; accepted 16 September 2002

Dedicated to Professor Jack Beauchamp on the occasion of his 60th birthday.

Abstract

The enthalpies for formation of nitric oxide (NO) upon protonation of gas-phase diazeniumdiolates were examined by combining the enthalpy for loss of two NO molecules from the ion, obtained from collision-induced dissociation (CID) threshold energy measurements, with the gas-phase acidity, $\Delta H_{acid}(R_2NH)$, of the corresponding amine. CID of the *N*-methylaniline-substituted diazeniumdiolate ion resulted in the formation of *N*-methylanilide anion by loss of two NO and the nitrosamine radical anion that results from single NO loss. Simultaneous modeling of the cross-sections for the two channels gave a $\Delta H_{298} = 1.23 \pm 0.17$ eV for loss of two NO molecules. From the dissociation energy of the ion and the gas-phase acidity of *N*-methylaniline, the enthalpy for formation of the amine and two NO molecules upon protonation of the diazeniumdiolate is determined to be -335.7 ± 4.4 kcal/mol. CID of the diethyl and piperidyl-substituted diazeniumdiolates gave NO^- and $N_2O_2^{\bullet -}$ ions in addition to the corresponding amide. Attempts to model the data to obtain dissociation energies were unsuccessful. Density functional calculations predict a small substituent effect on the enthalpy on formation of NO upon protonation of diazeniumdiolates in the gas phase, but little difference for the solvated ions. (Int J Mass Spectrom 222 (2003) 269–279)

Keywords: Nitric oxide; Diolate ions; CID; Protonation

1. Introduction

The development of prodrug analogs that release nitric oxide (NO) is of current interest because of NO's involvement in a variety of important bioregulatory processes, including blood pressure, neurotransmission, blood clotting, and immune-system control processes [1–5].

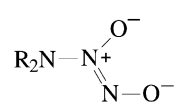

1

Diazeniumdiolate ions **1**, adducts of NO with secondary amines [6], are promising NO delivery agents because they have been found to spontaneously generate NO when dissolved in aqueous media [7–12]. The rates of release of NO from these compounds have been found to vary depending on their structure and the pH of the solution [8,13]. For example, NO

* Corresponding author. E-mail: pgw@purdue.edu

1387-3806/02/$ – see front matter
PII S1387-3806(02)00990-9

release from the ethyl-substituted diazeniumdiolate (R = ethyl) has been found to proceed faster than when R is a diamine or a triamine [13]. Recent experiments by Davies et al. [12] have found that the dissociations of these compounds are acid-catalyzed and it is proposed that equilibrium protonation precedes the release of NO, as shown in Eqs. (1) and (2).

$$\mathbf{1} \cdot H^+ \rightleftarrows \mathbf{1} + H^+ \quad (1)$$

$$\mathbf{1} \cdot H^+ \rightarrow R_2NH + 2NO \quad (2)$$

From their extensive kinetic studies, Davies et al. deduced that protonation at the R_2N nitrogen is what triggers dissociation of diazeniumidolates **1** to NO and amine at physiological pH [12].

In an attempt to investigate the origins of the rate dependence of NO release on the different substituents R in **1**, we sought to carry out measurements of the gas-phase energetics of NO generation from diazeniumdiolates by using the approach outlined in the thermochemical cycle shown in Eqs. (3)–(5). The enthalpy of reaction ($\Delta H_{rxn,298}$) for formation of NO upon protonation in the gas phase [Eq. (5)] can be determined by combining the bond dissociation enthalpy for NO loss from the ion [$\Delta H_{298}(R_2N–N(O)NO^-)$] obtained from collision-induced dissociation (CID) threshold energy measurements as shown in Eq. (3), with the gas-phase acidity, $\Delta H_{acid}(R_2NH)$, of the corresponding amine [Eq. (4)].

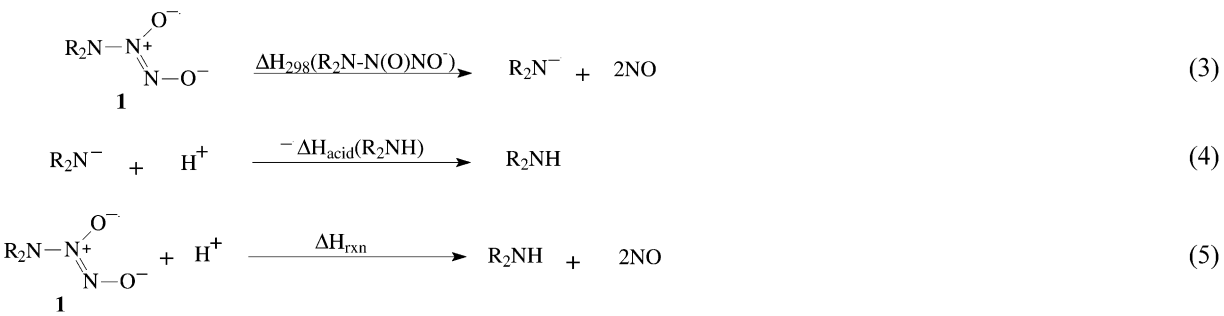

The derived $\Delta H_{rxn,298}$ obtained from this thermochemical cycle corresponds to the enthalpy of protonation of **1** at the nitrogen position and the resulting dissociation into the amine and two NO molecules. In this work, we have investigated the CID behavior for diazeniumdiolates **2–4**, and describe the determination of the enthalpy of NO formation upon protonation of the *N*-methylphenyl-substituted diazeniumdiolate **2**. The enthalpies of NO formation upon protonation of **2–4** are also examined using density functional theory, and compared to experimental results, where possible.

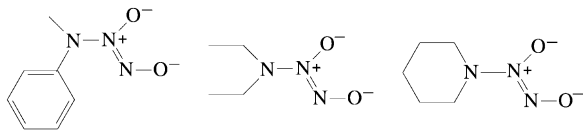

2. Experimental

2.1. Instrumental description

All the gas-phase experiments described in this paper were carried out in a flowing afterglow-triple quadrupole instrument described elsewhere [14,15]. For the present studies, helium buffer gas was maintained in the 1 m × 7.3 cm flow reactor at a total pressure of 0.4 Torr, with a flow rate of 200 STP cm^3/s and bulk flow velocity of 9700 cm/s. The primary reactant ion OH^- is produced by electron ionization of an N_2O/CH_4 mixture in the upstream end of the flow tube. Once formed, the ions are transported down the reactor by the flowing helium, where they are allowed to react with neutral reagent vapors introduced through leak valves. The ions in the flow tube, thermalized to ambient temperature by ca. 10^5 collisions with the helium buffer gas, are extracted from the flow

tube through a 1 mm orifice in a nose cone and are then focused into an EXTREL triple quadrupole analyzer.

CID studies are carried out by selecting the ions with the desired mass-to-charge ratio using the first quadrupole (Q1), and then injecting them into the second quadrupole (Q2, radio frequency only), where they undergo collision with argon target. For energy-resolved CID studies [16], the cross-sections for product formation are measured while the Q2 rod offset is scanned. The reactant and product ions are analyzed with the third quadrupole (Q3) and are detected with an electron multiplier operating in pulse counting mode. Absolute cross-sections are calculated using $\sigma_p = I_p/INl$, where I_p and I are the intensities of the product and reactant ions, respectively, N is the number density of the target, and l is the effective length of the collision cell, calibrated to be 24 ± 4 cm [15]. Unless specified otherwise, CID cross-sections are measured at different pressures and extrapolated to $p = 0$, such that they correspond to single collision conditions.

The center-of-mass collision energies are calculated using $E_{CM} = E_{lab}[m/(M + m)]$, where E_{lab} is the collision energy in the laboratory frame of reference, and m and M are the masses of the target and the ion, respectively. Determination of the ion kinetic energy origin and beam energy spread is accomplished by retarding potential analysis, with Q2 serving as the retarding field element. Ion beam energy distributions are found to be Gaussian in shape, with a typical full-width at half-maximum of 0.5–1.5 eV (laboratory frame).

2.2. Data analysis

Energy-resolved cross-sections are fit using the assumed model shown in Eq. (6) [16–20], where E is the energy of the ion, E_i is the vibrational energy, E_T is the dissociation energy, n is an adjustable parameter that reflects the energy deposition function for the collision between the ion and the target [21], and σ_o is a scaling factor.

$$\sigma(E) = \sigma_o \sum_i \left[\frac{g_i P_D(E, E_i, \tau)(E + E_i - E_T)^n}{E} \right] \quad (6)$$

Modeling is carried out by minimizing the deviation between the model function and the steeply rising portion of the appearance curve just above threshold. The ion energy distribution and Doppler broadening due to thermal motion of the target are also included in the fit.

Also incorporated into the analysis are the probabilities P_D of forming the product ions, which account for potential kinetic shifts that result from slow dissociation on the instrumental time scale (τ = ca. 30 μs) and competitive shifts that result when more than one ionic product is formed. For reactions that give only a single product, the probability depends only on the rate of ion dissociation. For CID processes that have more than one product, the probability for product formation also includes the branching ratio, calculated from the rates of the competing processes [22]. Ion dissociation rates and product branching ratios are calculated with RRKM theory. The transition states for simple dissociation reactions are calculated by using the procedures outlined by Rodgers et al. [23]. However, modeling the data for the loss of two free NO molecules [Eq. (5)] is more complicated. This reaction is a direct dissociation reaction and, therefore, a loose product-like transition state is expected, corresponding to the phase space limit [23]. At threshold, the products of the dissociation would be the amide ion and N_2O_2. However, because the 0 K bond dissociation energy in N_2O_2 is only 2–4 kcal/mol [24–28], dissociation to give two NO molecules is expected at energies only slightly above the threshold. Therefore, the reaction that occurs in the range that the data are fit will involve complete dissociation of the diazeniumdiolate into the amide ion and two neutral NO molecules. Unfortunately, the transition state for dissociation into an ion and two neutral products cannot be constructed by using phase space theory [29]. Therefore, single channel fits of the N_2O_2 loss cross-sections were carried out in two extremes. First, we modeled the data assuming formation of N_2O_2. This is the tight transition state limit because it is less entropically favored than the dissociation to give two NO molecules. To get the loose transition state limit, we assumed that the dissociation occurs completely on our experimental

time scale ca. 30 μs. The difference in CID threshold energies obtained from the two modeling limits depend on the magnitude of the dissociation energy, as ions with higher dissociation energies exhibit a larger difference between the two fitting approaches.

We have recently described an empirical approach to determine the transition state properties for a CID reaction that has competing channels [30]. Full fitting of a two-channel dissociation requires six parameters: σ_o, n, $E_0(1)$, $E_0(2)$, TS(1), and TS(2), where $E_0(1)$ and $E_0(2)$ and TS(1) and TS(2) are the dissociation energies and the transition state properties for channels 1 and 2, respectively. Observable physical parameters are the absolute maximum cross-sections for one of the channels, the partitioning between the two channels (branching ratio), the observed energy onsets for the two dissociation pathways, and the shapes (i.e., extent of curvature) of the curves. If at least one of the channels proceeds by direct dissociation, such that a variational transition state can be constructed, then there are five observable parameters and five unknowns, with a single set of optimal fitting parameters.

Because all the reactions examined in this work have multiple dissociation pathways, with one involving direct cleavage, the effective transition state properties for the N_2O_2 loss channel can in principle be determined empirically. The data are first fit by assuming loose transition states for all channels, with frequencies equal to those in the products. For loss of N_2O_2, the products are the amide ion and N_2O_2. The fit is then improved by adjusting the low-energy frequencies for the N_2O_2 loss transition state so to reproduce the branching ratios for the products over the fitting range, which is chosen so to include the steeply rising regions of all the appearance curves included in the fit. In this work, that also includes regions of the competing channels where the cross-sections are nearly zero, or invariant with energy. The approach described here for systems where the transition state properties are not all known is an alternative to the "independent scaling" method used by Rodgers and Armentrout [22] and Amicangelo and Armentrout [31]. Although the empirically determined activation entropy likely reflects the partition function for the transition state, the actual frequencies for the transition state most likely do not agree with those used here.

Physical parameters for the reactants and products, including vibrational frequencies, rotational constants, and polarizabilities, are calculated at the Becke3LYP/6-31+G* (B3LYP/6-31+G*) level of theory [32]. Experimental N_2O_2 frequencies [33] are used in the modeling because B3LYP fails to describe the elongated and weakly bound NO dimer [34,35]. Calculated vibrational frequencies are scaled by 0.965 to account for anharmonicities, unless specified otherwise. Dissociation energies obtained from the fitting procedures correspond to the 0 K energies, and are converted to the 298 K bond dissociation enthalpies, ΔH_{298}, using the integrated heat capacities for the reactants and products obtained from the scaled, calculated frequencies. All CID data analysis is carried out using the CRUNCH program developed by Armentrout and co-workers [17–19,22].

2.3. Materials

The procedure for the preparation of O^2-alkyl-(*N*,*N*-alkylamino)diazen-1-ium-1,2-diolates has been previously described [11]. O^2-Ethyl-1-(*N*-methyl-*N*-phenylamino)diazen-1-ium-1,2-diolate **4** was prepared by coupling the novel 1-(*N*-methyl-*N*-phenylamino)diazen-1-ium-1,2-diolate with ethyliodide using standard protocol [11]. Full characterization of the solution chemistry of this diazeniumdiolate and its O^2-ethyl derivative **5** are currently underway. All other reagents were obtained from commercial sources and were used as supplied. Gas purities were as follows: He (99.995%), NO_2 (99.5%), and CH_4 (99%).

3. Results

The following sections describe the results of the studies of the heats of protonation of the three diazeniumdiolates, **2**−**4**. We first describe CID results for the three compounds and use those results, where

possible, to calculate of the heat of reaction for NO generation from all three compounds. In the last section, the experimental results are discussed in light of theoretical predictions.

3.1. CID measurements

Diazeniumdiolate ions **2**–**4** were synthesized in the gas phase by an E2 elimination reaction of the corresponding O^2-alkylated diazeniumdiolate derivatives **5** with hydroxide or fluoride ions, as shown in Eq. (7). Four reaction pathways are observed upon CID of the ions, as shown in Eqs. (8)–(10).

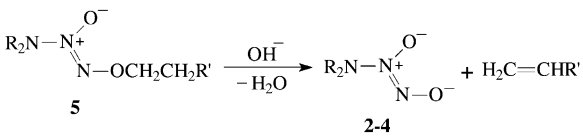

(7)

All three ions lose the equivalent of two NO molecules upon CID to form an R_2N^- ion [Eq. (3)]. However, for the alkyl-substituted ions (**3** and **4**), the $N_2O_2^{\bullet -}$ ion is also observed as a major fragment, and the corresponding neutral fragment is likely the amino radical. The formation of $N_2O_2^{\bullet -}$ in these reactions suggests that the adiabatic electron affinity of N_2O_2 is comparable to those for the amino radicals (the vertical detachment energy of $N_2O_2^{\bullet -}$ is much higher, ~3 eV [36]). Alkyl-substituted amino radicals have electron affinities of ca. 0.7–0.8 eV [36]. The $N_2O_2^{\bullet -}$ ion is not observed upon CID of the *N*-methylaniline derivative **2** consistent with the fact that the electron affinities of anilino radicals are ca. 1 eV higher than those for the alkyl-substituted radicals [36].

All three ions also lose NO upon CID. For the alkyl-substituted ions, the electron stays with the NO to give NO^-, but for the aniline derivative the product is the radical anion of the nitrosamine **6**, $C_6H_5N(CH_3)NO^{\bullet -}$. The difference can be attributed to the differences in electron affinities of the nitrosamine products. Calculations at the B3LYP/6-31+G* level of theory carried out in this work predict the diethylnitrosamine radical anion, $(C_2H_5)NNO^{\bullet -}$, to be unbound with respect to electron attachment by ~5 kcal/mol, while methylphenylnitrosamine, $C_6H_5N(CH_3)NO$, is calculated to have an electron affinity of ca. 20 kcal/mol. The electron affinity of NO is 0.68 kcal/mol [36].

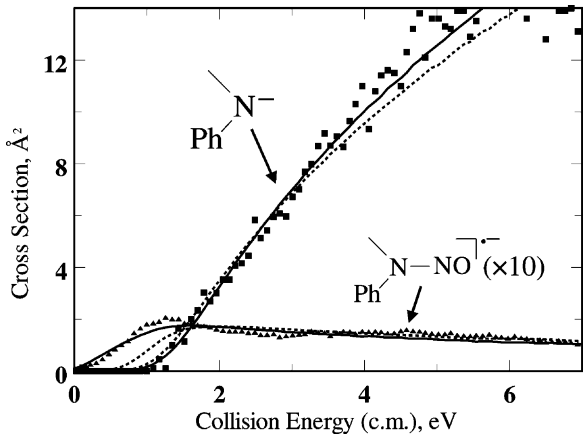

Fig. 1. Cross-sections for formation of **2a** and **6** upon CID of ion **2** with Ar target. The dashed and solid lines are the fits obtained using loose and tight transition states for the formation of **6**, respectively, and a very loose transition state for formation of **2a**.

Energy-resolved cross-sections for CID of the three diazeniumdiolates are shown in Figs. 1–3. Details of the CID spectra and the modeling are described in the following sections.

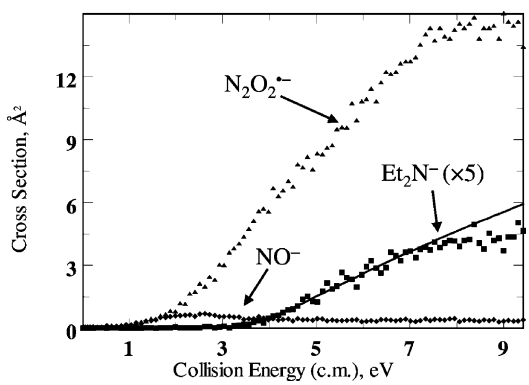

Fig. 2. Cross-sections for formation of **3a**, NO^-, and $N_2O_2^{\bullet -}$ upon CID of **3** with Ar target. The solid line is the fit of the **3a** cross-section data using the loose transition state model, as described in the Section 2.2.

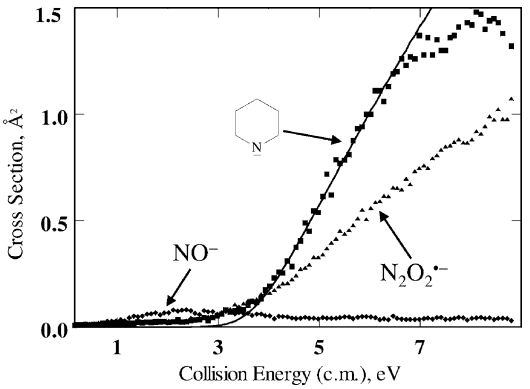

Fig. 3. Cross-sections for formation of **4a**, NO^-, and $N_2O_2^{\bullet -}$ upon CID of **4** with Ar target. The solid line is the fit of the **4a** cross-section data using the loose transition state model, as described in the Section 2.2.

3.1.1. *N*-Methylaniline derivative **2**

CID of ion **2** results in the formation of *N*-methylanilide ion **2a** and the nitrosamine anion **6** that results from NO loss [Eq. (8)]. The cross-sections for formation of the products as a function of center-of-mass collision energy are shown in Fig. 1. The onset for the formation of **6** is lower in energy than that for formation of **2a**, but at high energy the *N*-methylanilide is the predominant product.

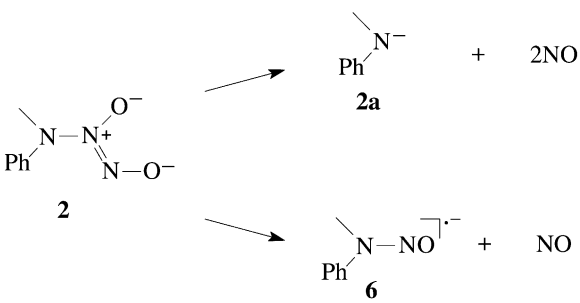

(8)

We initially fit the cross-sections for **2a** ignoring the competition with the second dissociation channel. Modeling of the data using the tight and loose transition state limits as described in the data analysis section gives 298 K bond dissociation energy values of 1.31 and 1.32 eV, respectively, with n values of 1.4 ± 0.1. The average of these two values is 1.32 ± 0.17 eV, where the uncertainty includes the standard deviation of values from replicate data sets, a 0.15 eV (laboratory frame) uncertainty in the absolute energy scale, and a 0.01 eV contribution due to the uncertainty in the transition state. This value should be considered an upper limit to the dissociation energy because the value is subject to a competitive shift.

To account for the potential competitive shift, we also fit the two channels simultaneously using the procedures described by Rodgers and Armentrout [22]. Transition states for the dissociation reactions were created by adjusting the five lowest frequencies for the variational transition states to obtain the best fit of the data. The only way to fit the cross-sections for formation of **2a** when considering the second channel was to use an exceptionally loose transition state, where the bottom five vibrational frequencies have values that are $<15\,cm^{-1}$. The resulting activation entropy is ca. 80 eu, which is much higher than those for most simple dissociation reactions involving the formation of an ion and a single neutral product [20,37–40]. Tighter transition states for formation of **2a** lead to worse agreement between the data and the model, regardless of the transition state chosen for formation of nitrosamine ion. In the initial fitting, the formation of **6** was assumed to occur through a loose, product-like transition state. The fit obtained using these transition state properties and a fitting range of ca. 0–4 eV is shown as the dashed line in Fig. 1. For this fit, the threshold energy for formation of the nitrosamine ion was 1.06 eV, and $n = 1.4 \pm 0.1$. The onset for formation of **2a** gives $\Delta H_{298}(\mathbf{2}) = 1.20$ eV (27.7 kcal/mol). Although the cross-sections for the formation of **2a** are reasonably reproduced by the model, the fit for the nitrosamine ion cross-sections misses the onset region completely. In order to improve the fit, the transition state for the nitrosamine ion channel had to be tightened significantly by increasing the frequencies and rotational constants. The fit shown as the solid line in Fig. 1 was obtained by using the same fitting range with a threshold of 1.26 eV for the formation of **2a** (which corresponds to $\Delta H_{298}(\mathbf{2}) =$

29.1 kcal/mol), a threshold of 0.28 eV for the formation of **6**, and $n = 1.5 \pm 0.1$. However, this fit was obtained using an unrealistically tight transition state for the formation of the nitrosamine ion, with an activation entropy of ca. −20 eu. Although it is not surprising that the transition state does not have a simple, product-like structure, as the formation of the open-shell ion is formally symmetry forbidden, the activation entropy is more consistent with that expected for significant geometric rearrangement. Fortunately, although the transition states for formation of the nitrosamine ion leading to the two fits are significantly different, the difference in the threshold energies for formation of **2a** under these two extreme conditions is only 0.06 eV. Therefore, the final assigned value for the dissociation energies is chosen as the average of the two extremes, 1.23 ± 0.17 eV (28.4 ± 3.9 kcal/mol), where the uncertainty again includes the standard deviation of values from replicate data sets, and a 0.15 eV (laboratory) contribution due to uncertainty in the absolute energy scale, but also includes an extra 0.03 eV to account for uncertainty in the transition state of the nitrosamine ion channel.

To summarize, modeling of the cross-sections for dissociation of **2** required a very loose transition state for formation of **2a**, consistent with formation of **2a** and two NO molecules, but modeling the cross-sections for formation of the nitrosamine ion required a very tight transition state. However, the choice of transition state for formation of **6** has only a small effect on the measured onset for formation of **2a**. The competitive shift for the onset of **2a** is found to be less than 0.10 eV.

3.1.2. *N,N-Diethylamine derivative **3***

Reaction of the O^2-propyl diazeniumdiolate **5** (R′ = Me), derived from *N,N*-diethylamine, with hydroxide ion results in the formation of the diazeniumdiolate ion **3** by E2 elimination and/or substitution. CID of the ion [Eq. (9)] produces the diethylamide ion at *m/z* 72, but only as a minor product over all energies (Fig. 2). The NO ion, NO^-, is also observed, but the most abundant product at high energies is the $N_2O_2^{\bullet -}$ ion.

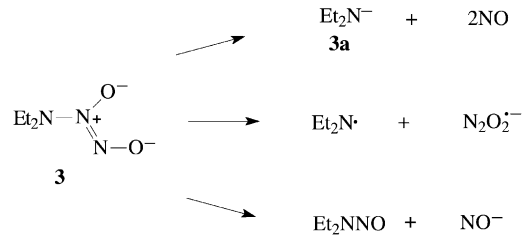

(9)

Attempts to fit the cross-sections for the three products simultaneously were unsuccessful. During these attempts, the transition state for formation of NO^- was restricted to a loose, product-like structure whereas the transition states for formation of **3a** and $N_2O_2^{\bullet -}$ were adjusted freely. However, no combination of transition state properties could be found that would accurately reproduce the cross-sections for formation of **3a** and $N_2O_2^{\bullet -}$. By using a single channel fit (solid line, Fig. 2) with in the loose transition state limit, we obtain an upper limit of 3.52 eV (81.2 kcal/mol). However, because of the low-energy channels, this onset is likely subject to a large competitive shift.

3.1.3. *Piperidine derivative **4***

CID of the piperidine-derived diazeniumdiolate **4** gives the ionic products NO^-, $N_2O_2^{\bullet -}$, and $C_5H_{10}N^-$ **4a** [Eq. (10)]. The observed products are analogous to those observed with the diethylamine derivative **3** which is not surprising considering the similarity of the substituents.

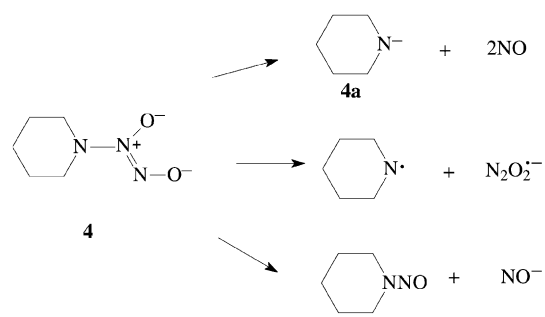

(10)

However, there are significant differences in the energy dependences of the cross-sections (Fig. 3). Unlike

what was found for the diethylamine derivative, the yield of the amide ion is greater than that for $N_2O_2^{\bullet-}$ over most of the energy range examined. The origins of the differences in the energy dependences are not clear. A large difference in electron affinities of the diethylamino and piperidyl radicals would account for the difference in the cross-sectional data, but calculations at the B3LYP/6-31+G* level of theory predict only a small (∼1 kcal/mol) difference in the electron affinities of the two radicals. Another possible explanation for the large difference in the cross-section energy dependence for the diethylamine and piperidine derivatives is the difference in transition states for the two systems. This assessment is supported by theoretical calculations. The activation entropy for formation of $N_2O_2^{\bullet-}$ from ion **3** is calculated in the phase space limit to be ca. 4 eu higher than that for formation of $N_2O_2^{\bullet-}$ from ion **4**, whereas the activation entropies for the formation of the neutral N_2O_2 molecule agree to within 1 eu. Therefore, despite the fact that the dissociation energies for the two ions are similar, the dissociation of $N_2O_2^{\bullet-}$ from **4** occurs more slowly, and is, therefore, subject to larger kinetic and competitive shifts.

As with the diethyl derivative, we were unable to model simultaneously the cross-sections for all three ionic products. A single channel fit gives a value of 3.46 eV (79.9 kcal/mol), which is again expected to be shifted significantly due to the competitive dissociation.

3.2. Protonation enthalpy

The enthalpy change for the loss of two NO molecules upon protonation of diazeniumdiolate **2** was obtained via the thermochemical cycle of Eqs. (3)–(5) and is listed at the bottom of Table 1. Formation of NO upon protonation of diazeniumdiolates in the gas phase is highly exothermic because of charge neutralization. Because we were unable to model completely the data for the dissociation of **3** and **4**, the enthalpies for formation of NO upon protonation of those ions are not calculated.

Table 1
Measured and derived thermochemical data (in kcal/mol)[a]

Parameter	Value	Reference
Ion dissociation energies[b]		
ΔH_{298}(**2**)	29.1 ± 3.9	This work
n[a]	1.4 ± 0.1	
ΔH_{298}(**3**)	≤81.2	This work
n[a]	1.5 ± 0.1	
ΔH_{298}(**4**)	≤79.9	This work
n[a]	1.5 ± 0.1	
Gas-phase acidities		
N-Methylaniline	364.8 ± 2.1	[36]
Reaction enthalpies[c]		
$-\Delta H_{rxn,298}$(**2**)	335.7 ± 4.4	Experiment, this work
	323.0	Calculated, Method I
	327.9	Calculated, Method II
$-\Delta H_{rxn,298}$(**3**)	325.2	Calculated, Method I
	330.1	Calculated, Method II
$-\Delta H_{rxn,298}$(**4**)	329.0	Calculated, Method I
	333.9	Calculated, Method II

[a] Exponent in Eq. (6).
[b] 298 K enthalpy for dissociation of the diazeniumdiolate ion to give two NO molecules [Eq. (3)].
[c] Exothermicity of NO formation upon protonation of **2**–**4**. Values correspond to $-\Delta H_{rxn}$ for Eq. (5).

3.3. Computational results

Density functional calculations were carried out to obtain molecular parameters for the fitting and to get theoretical predictions for the energies measured in this work. Energies for all species calculated at the B3LYP/6-31+G* level of theory are listed in Table 2. Optimized geometries and vibrational frequencies for all of the species at the B3LYP/6-31+G* level of theory are available from the authors.[1]

The calculated energies can be used to calculate the enthalpy for NO generation upon protonation of ions **2**–**4**. Enthalpies of reaction for the process shown in Eq. (5) have been calculated using two approaches. In the first (Method I), the enthalpy was calculated directly, using the 298 K enthalpies of the reactants and products. The results are summarized in Table 1. However, because of the differences in electronic

[1] Available on the World Wide Web at http://www.chem.purdue.edu/wenthold/.

Table 2
Calculated energies[a] for diazeniumdiolates, amines, and deprotonated amines examined in this work, in the gas phase and in aqueous solution[b]

	Gas phase	Aqueous solution
2	−586.17937	−586.28257
3	−473.05171	−473.15809
4	−511.16154	−511.26995
2a	−326.33128	
3a	−213.17239	
4a	−251.27901	
Diethylamine	−213.80554	−213.81143
Piperidine	−251.91270	−251.92113
N-Methylaniline	−326.92366	−326.93498

[a] For optimized geometries at the B3LYP/6-31+G* level of theory; values in Hartrees.
[b] Solution energies calculated using the PCM approach [42].

structure between the reactants and products a second approach shown in Eq. (11) has been utilized (Method II), where we calculate the enthalpy for formation of N_2O_2, and then add the 298 K bond dissociation enthalpy of N_2O_2, ca. 1 kcal/mol [24–28].

2-4

(11)

There is a difference in the calculated enthalpies from the two approaches because density functional theory does not give an accurate bond dissociation enthalpy for N_2O_2, attributed to an improperly balanced description of static and dynamic electron correlation contributions [35]. Of the two approaches, Method II gives a result that is in better agreement with the measured protonation enthalpy for ion **2**, while that calculated with Method I differs by ca. 12 kcal/mol from the experimental result, suggesting that Method II provides a more balanced treatment of correlation energy for this system. However, the calculated enthalpy obtained by using Method II is still in very poor agreement with the experimental result.

Table 3
The effect of substituent polarizability on enthalpy of NO formation upon protonation of diazeniumdiolates

Substituent	Relative enthalpies[a] (kcal/mol)		Amine polarizability[b] (Å^3)
	Gas phase	Aqueous[c]	
$Ph(CH_3)N$–	0.0	0.0	13.3
Et_2N–	6.0	0.6	9.7
$C_5H_{10}N$–	2.2	−0.8	10.8

[a] Theoretical values, calculated at the B3LYP/6-31+G* level of theory. Corresponds to $-\Delta H$ for the reactions shown in Eqs. (12a) and (12b). The larger value indicates that protonation is more exothermic.
[b] Polarizability of the amine that corresponds to substituent, calculated from group additivity increments [41].
[c] Calculated at the B3LYP/6-31+G* level of theory, including the PCM treatment of solvation [42] with water solvent.

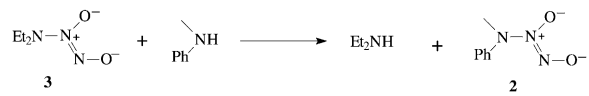

3 **2**

(12a)

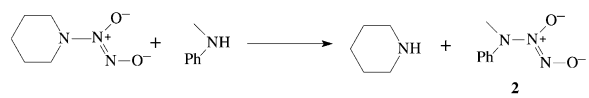

4 **2**

(12b)

The relative enthalpies for NO formation for the ions can be calculated by using Eqs. (12a) and (12b). This approach should be more reliable than the absolute methods because it does not consider the structure of the N_2O_2 products. The calculations predict that formation of NO from the aniline derivative **2** should be the least exothermic process, while formation of NO from **3** and **4** is more exothermic ($-\Delta H$ for Eq. (5) is larger) by 6.0 and 2.2 kcal/mol, respectively. Therefore, the calculations predict a small substituent on the enthalpy for formation of NO upon protonation of diazeniumdiolates in the gas phase. The calculated relative energies are consistent with the expected stability of the ions given the size of the amine substituent, where the larger substituents are better able to stabilize the negative charge. This is illustrated by the data shown in Table 3, which lists the relative reaction enthalpies for **2**–**4** and the polarizabilities [41]

of the amines from which the diazeniumdiolates are derived. The observed trend indicates that NO generation is less exothermic for gaseous ions with larger substituents.

In order to investigate the effect of solvation, the enthalpies of the reactions in Eqs. (12a) and (12b) were recalculated by using the Polarized Continuum Model (PCM) [42], in which the molecular cavity in a dielectric continuum is approximated by using overlapping spheres around atoms. The PCM approach is expected to be more accurate than the Onsager model [43] which uses a spherical molecular cavity. It is likely less accurate than an isodensity PCM [44], where the molecular cavity is calculated in a self-consistent fashion, but is significantly cheaper computationally. The solution-phase energies for the species in Eqs. (12a) and (12b) are listed in Table 2, and the calculated reaction enthalpies are in Table 3. When solvation is included, the differences between the protonation enthalpies are significantly smaller, and do not show a discernible trend. Presumably, the presence of a counter-ion in solution will also affect the energetics of the protonation reaction.

The enthalpy of NO formation upon protonation of diazeniumdiolates has not been addressed in previous computational studies, which have focused on the effect of substituents on the geometry and electronic structure of **1** [45]. In that work, it was shown that the two oxygen atoms in diazeniumdiolates have the bulk of the negative charge, nearly equally distributed between them, which led the authors to postulate that diazeniumdiolates could be equally protonated at either of those atoms. However, the study did not consider the protonation at the amine nitrogen [12].

4. Conclusion

The dissociation of diazeniumdiolates **1** in the gas phase proceeds by four pathways, giving amide ion (R_2N^-), $N_2O_2^{\bullet -}$, $R_2NNO^{\bullet -}$, and NO^-, and the amount of each product depends on the thermochemical properties and structures of the ions and neutral products that are formed. Amide ion formation is most prevalent for systems where the ion has a large electron binding energy, such as the case for an anilide ion, whereas $N_2O_2^{\bullet -}$ is more likely to be formed for ions with low electron binding energies, such as alkyl-substituted amide ions.

Modeling the cross-sections for dissociation of the *N*-methylanilino-substituted diazeniumdiolate **2** indicates a loose transition for loss of N_2O_2, consistent with the formation of two NO molecules and amide ion. The dissociation energy for formation of amide ion and two NO molecules is used to determine the enthalpy for formation of NO upon protonation of the diazeniumdiolate. Formation of NO and amine upon protonation of diazeniumdiolates in the gas phase is a highly exothermic process, as expected for a charge neutralization process. Modeling the competition between formation of amide ion and $N_2O_2^{\bullet -}$ was found to be challenging, likely because of the large differences in the transition states for the two processes. As a result, only limits to the thermochemical properties could be obtained for systems that gave $N_2O_2^{\bullet -}$ as a dissociation product. Density functional calculations predict that larger, more polarizable substituents decrease the exothermicity of the gas-phase reaction, presumably by stabilizing the negative ion. However, the effect of substitution on the energetics for NO formation upon protonation is much smaller when solvation is included in the calculations. These results highlight the fact that solution-phase trends in energies do not necessarily mirror those obtained for gas-phase calculations.

Acknowledgements

We thank the donors of the Petroleum Research Fund, administered by the American Chemical Society for support of work at Purdue, and the National Institutes of Health (R01 GM58109) for support of the work at Johns Hopkins. We also thank Dr. Larry Keefer of the National Cancer Institute for useful discussion about the properties and reactivity of diazeniumdiolates.

References

[1] S. Moncada, E.A. Higgs, FASEB J. 9 (1995) 1319.
[2] S. Moncada, R.M.J. Palmer, E.A. Higgs, Pharmacol. Rev. 43 (1991) 109.
[3] L.J. Ignarro, G.M. Buga, K.S. Wood, R.E. Byrns, G. Chaudhuri, Proc. Natl. Acad. Sci. U.S.A. 84 (1987) 9265.
[4] A.R. Butler, D.L.H. Williams, Chem. Soc. Rev. 22 (1993) 233.
[5] P.L. Feldman, O.W. Griffith, D.J. Stuehr, J. Chem. Eng. News Dec. 20 (1993) 26.
[6] R.S. Drago, Reactions of nitrogen(II) oxide, in: C.B. Colburn (Ed.), Free Radicals in Inorganic Chemistry, American Chemical Society, Washington, DC, 1962.
[7] S.R. Hanson, T.C. Hutsell, L.K. Keefer, D.L. Mooradian, D.J. Smith, Adv. Pharmacol. (San Diego) 34 (1995) 383.
[8] L.K. Keefer, R.W. Nims, K.M. Davies, D.A. Wink, Methods Enzymol. 268 (1996) 281.
[9] L.K. Keefer, CHEMTECH 28 (1998) 30.
[10] L.K. Keefer, Pharm. News 7 (2000) 27.
[11] A. Srinivasan, N. Kebede, J.E. Saavedra, A.V. Nikolaitchik, D.A. Brady, E. Yourd, K.M. Davies, L.K. Keefer, J.P. Toscano, J. Am. Chem. Soc. 123 (2001) 5465.
[12] K.M. Davies, D.A. Wink, J.E. Saavedra, L.K. Keefer, J. Am. Chem. Soc. 123 (2001) 5473.
[13] C.M. Maragos, D. Morley, D.A. Wink, T.M. Dunams, J.E. Saavedra, A. Hoffman, A.A. Bove, L. Isaac, J.A. Hrabie, L.K. Keefer, J. Med. Chem. 34 (1991) 3242.
[14] S.T. Graul, R.R. Squires, Mass Spectrom. Rev. 7 (1988) 1.
[15] P.J. Marinelli, J.A. Paulino, L.S. Sunderlin, P.G. Wenthold, J.C. Poutsma, R.R. Squires, Int. J. Mass Spectrom. Ion Processes 130 (1994) 89.
[16] P.B. Armentrout, J. Am. Soc. Mass Spectrom. 13 (2002) 419.
[17] K.M. Ervin, P.B. Armentrout, J. Chem. Phys. 83 (1985) 166.
[18] R.H. Schultz, K.C. Crellin, P.B. Armentrout, J. Am. Chem. Soc. 113 (1991) 8590.
[19] N.F. Dalleska, K. Honma, L.S. Sunderlin, P.B. Armentrout, J. Am. Chem. Soc. 116 (1994) 3519.
[20] K.M. Ervin, Chem. Rev. 101 (2001) 391.
[21] F. Muntean, P.B. Armentrout, J. Chem. Phys. 115 (2001) 1213.
[22] M.T. Rodgers, P.B. Armentrout, J. Chem. Phys. 109 (1998) 1787.
[23] M.T. Rodgers, K.M. Ervin, P.B. Armentrout, J. Chem. Phys. 106 (1997) 4499.
[24] S.G. Kukolich, J. Mol. Spectrosc. 98 (1983) 80.
[25] J.R. Hetzler, M.P. Casassa, D.S. King, J. Phys. Chem. 95 (1991) 8086.
[26] A. Dkhissi, P. Soulard, A. Perrin, N. Lacome, J. Mol. Spectrosc. 183 (1997) 12.
[27] I. Fischer, A. Strobel, J. Staecker, G. Niedner-Schatteburg, K. Müller-Dethlefs, V.E. Bodybey, J. Chem. Phys. 96 (1992) 7171.
[28] C.E. Dinerman, G.E. Ewing, J. Chem. Phys. 53 (1970) 626.
[29] P. Pechukas, J.C. Light, J. Chem. Phys. 42 (1965) 3281.
[30] I.H. Krouse, H.A. Lardin, P.G. Wenthold, Int. J. Mass Spectrom. Ion Processes (2002) in press.
[31] J.C. Amicangelo, P.B. Armentrout, Int. J. Mass Spectrom. 212 (2001) 301.
[32] M.J. Frisch, G.W. Trucks, H.B. Schlegal, P.M.W. Gill, B.G. Johnson, M.A. Robb, J.R. Cheeseman, T. Kieth, G.A. Petersson, J.A. Montgomery, K. Raghavachari, M.A. Al-Laham, V.G. Zakrewski, J.V. Ortiz, J.B. Foresman, J. Cioslowski, B.B. Stefanov, A. Nanayakkara, M. Challacombe, C.Y. Peng, P.Y. Ayala, W. Chen, M.W. Wong, J.L. Andres, E.S. Replogle, R. Gomperts, R.L. Martin, D.J. Fox, J.S. Binkley, D.J. Defrees, J. Baker, J.J.P. Stewart, M. Head-Gordon, C. Gonzalez, J.A. Pople, Gaussian 98, Revision C.3, Pittsburgh, PA, 1998.
[33] A.R.W. McKellar, J.K.G. Watson, B.J. Howard, Mol. Phys. 86 (1995) 273.
[34] J.K. Park, H. Sun, Chem. Phys. 263 (2001) 61.
[35] A. Snis, I. Panas, Chem. Phys. 221 (1997) 1.
[36] J.E. Bartmess, Negative ion energetics data, in: W.G. Mallard, P.J. Linstrom (Eds.), NIST Chemistry WebBook, NIST Standard Reference Database Number 69, National Institute of Standards and Technology, Gaithersburg, MD, 2000, p. 20899 (http://webbook.nist.gov).
[37] P.G. Wenthold, J. Phys. Chem. A 104 (2000) 5612.
[38] J. Laskin, B. Hadas, T.D. Mark, C. Lifshitz, Int. J. Mass Spectrom. 177 (1998) L9.
[39] M. Oblinger, A.J. Lorquet, J.C. Lorquet, Int. J. Mass Spectrom. Ion Processes 167/168 (1997) 149.
[40] Y. Gotkis, M. Naor, J. Laskin, C. Lifshitz, J.D. Faulk, R.C. Dunbar, J. Am. Chem. Soc. 115 (1993) 7402.
[41] K.J. Miller, J. Am. Chem. Soc. 112 (1990) 8533.
[42] S. Miertus, E. Scrocco, J. Tomasi, Chem. Phys. 55 (1981) 177.
[43] L. Onsager, J. Am. Chem. Soc. 58 (1936) 1486.
[44] J.B. Foresman, T.A. Keith, K.B. Wiberg, J. Snoonian, M.J. Frisch, J. Phys. Chem. 100 (1996) 16098.
[45] D.K. Taylor, I. Bytheway, D.H.R. Barton, C.A. Bayse, M.B. Hall, J. Org. Chem. 60 (1995) 435.